Irinotecan Loaded Lipomers: Development, And Characterization For Proof of Concept To Combat Colon Cancer

Prabhanjan S Giram (prabhanjanpharma@gmail.com)
CSIR-National Chemical Laboratory https://orcid.org/0000-0003-0439-1347
Baijayantimala Garnaik
CSIR-National Chemical Laboratory

Research Article

Keywords: Colon cancer, Irinotecan, Lipomers, Neutropenia, Chemotherapy, PLGA.

Posted Date: November 1st, 2021

DOI: https://doi.org/10.21203/rs.3.rs-909391/v1

Abstract

PLGA Poly (lactide-co-Glycolide) is a biocompatible and biodegradable copolymer gained popularity for tissue engineering, drug delivery, biosensing, and biomedical applications. In the present study PLGA of (M_w =13,900) has synthesized by ring opening polymerization with zinc proline initiator. Irinotecan (Ir) loaded Lipomers (LPs) formulated with PLGA, DSPE-PEG (2000) (1,2-distearoyl-sn-glycero-3-phosphoethanolamine-N-[amino (polyethylene glycol)-2000) and soya lecithin excipients by nanoprecipitation method. These formulated LPs further validated by physicochemical and biological potential for colon delivery applications. The potential of LPs for delivery of Irinotecan (Ir), a poorly water-soluble chemotherapeutic drug used for the treatment of colon cancer was studied. LPs of controlled size (80-120 nm), surface charge (~ -35 mV), sustained release potential and significant cytotoxicity against CT-26 (colon) cancer cells, were successfully prepared. *In-vivo* biodistribution and tumor site retention in CT-26 xenografts tumor bearing Balb/C mice showed promising result for tumor uptake and retention for prolong time period. Unlike P-DSPE-Ir, PEG coated P-DSPE-PEG-Ir LPs exhibit significant tumor growth delay compared to untreated and blank formulation treated groups in the CT-26 subcutaneous tumor model, after 4 treatments of 10 mg Ir/kg dose. The biocompatibility, safety of LPs confirmed by acute toxicity study of optimized formulation. Overall, this proof-of-concept study demonstrates that the LPs improved efficacy, bioavailability and decreases neutropenia of Ir to combat colon cancer.

1. Introduction

PLGA is most commonly used biocompatible, non-toxic, biodegradable and non-immunogenic polymer of 21 st Centuary.PLGA synthesized by using ring-opening polymerization (ROP) of lactide, glycolide with suitable catalyst to overcomes ring strain of lactones. In this polymerization method mostly tin based stannous octoate, enzymatic, organocatalysis, carbene as well as nucleophilic catalyst made significant contributions [1]. These catalysts show pros and cons in ROP. PLGA copolymers have been extensively used in the fields of drug delivery for various applications such as [2], tissue engineering [3-4], medical devices [5], and single-use plastics [6]. Synthesis of PLGA carried with stannous octoate, as a techno commercially catalyst [7]. However, use of tin-based catalysts showed broad polydispersity (PDIs), has toxicity issue and more readily trans esterified PLGAs are formed, which is not considered good sign for its different application [8]. DBU catalyst provides random copolymer of PLGA with sequential addition of glycolide into the reactor, upon addition of Initiator alcohols and shows toxicity at higher concentration [1]. To avoid all these toxicity issues of catalysis for drug delivery application. There is growing interest for zinc-based catalyst used due to its biocompatible nature. Zinc proline is biocompatible metal amino acid complex available in the FDA approved immunological tincture [9]. In recent year, nanomedicine has been successfully translated various commercial products, from the lab to the clinical market. It provides significant improvement in patients life expectancy and new solutions in the form of pharmaceutical innovation with lower cost, lower risks to patients and much higher efficiency as compared to traditional products [10]. Nanocarrier based drug delivery formulations improve the bioavailability, pharmacokinetics profile, minimise side effects, and protects anticancer agents from biological system for better

therapeutic effects [11].Nanoformulation includes nanoparticles, liposome, nanosuspensions, lipid polymer hybrid nanoparticles also called as LPs.These LPs perform better in the clinical application because of improved stability of therapeutic agents against chemical as well as enzymatic degradation [12-14]. LPs is lipid polymer hybrid carrier for drug delivery has advantages of both lipid and polymer for stability and biocompatibility [15]. LPs combines mechanical advantages of polymeric core, biocompatible and biodegradable phospholipids shell into a single platform. LPs contains hydrophobic polymeric core such as poly (lactic acid) (*PLA*), poly(e-caprolactone) (PCL) and PLGA which is capable of encapsulating the sparingly water-soluble drugs with higher loading efficiency as compared to polymeric nanoparticles. Shell is made from phospholipids like DSPE, DSPE-PEG (2000) to provide stealth properties for nanocarriers. Soya lecithin layer act as fence between these core-shell layer, performs two major functions such as a biocompatible shield and barrier for preventing fast leakage of water-soluble drugs from LPs [16-17]. The pitfalls of liposome easily clearance from reticuloendothelial system (RES), lack of structural integrity, stability issue, drug crystallization, and occurrence of polymorphic changes upon storage [18-19]. Nowadays, Cancer is the second leading cause of death worldwide and responsible for 8.8 million deaths in 2015 [20]. To treat colon cancer and prevent remission, various types of anticancer agents such Irinotecan,5-flurouracil, gemcitabine loaded with biocompatible and biodegradable polymers such as PLA, PLGA, PCL, Methoxy terminated poly (L-Lactide-co Glycolide) (m-PEG-PLGA) and Chitosan for better chemotherapy [21]. Ir is BCS-II drug act on topoisomerase 1 which results DNA damage and cell death. Ir is poorly soluble in the water, there is scientific quest to improve its delivery to cancer cell [22]. Genexol-PM consists micelles of 20–50 nm with m-PEG-PLA core containing paclitaxel [23]. Cisplatin has been incorporated into polyethylene glycol (PEG)-poly (amino acid) block copolymer micelles [24-25]. In 2015, the U.S. Food and Drug Administration (FDA) have already approved Ir liposome (Onivyde®) for treating patients with metastatic pancreatic cancer [26]. Doxil® approved to the U.S. market in 1995 for the treatment of patients with ovarian cancer and AIDS-related Kaposi's sarcoma [27-29]. The progress in the liposome technology has also shown the emergence of the next generation of lipid-based LPs, including solid lipid LPs, nanostructure lipid carriers, and lipid-polymer hybrid LPs, which may overcome the current drawbacks encountered by both liposome and polymeric nanoparticles [30-33]. In the literature Mori al., reported LL-37 antimicrobial peptide conjugated with carboxyl group of PLGA and results in the formation of micelles. These micelles showed excellent physicochemical properties of particle size 50-70 nm, zeta potential (10-20 mV) stability and In-vitro cell viability significantly reduced with IC_{50} (10-25uM) as compared with standard LL-37 peptide IC_{50} (100-130 Um) tested against HM-1, B16/BL6, HeLa, and HepG2 cell lines [34].In another report thymoquinone loaded lipid-polymer nanocarriers of PLGA, phosphatidylcholine to improve anticancer oral delivery of doxorubicine using co-delivery approach proved significant difference in cell viability study of lipid-polymer nanocarriers loaded with two drugs[35].Wang et.al.,reported PLGA nanocarriers loaded doxorubicine with surface functionalized performed using polyethylene glycol and active targeting ligand RGD to achieve efficient active passive targeting for malignant cancer. These nanocarriers showed better physicochemical and biological properties for anticancer applications [36]. Zhang et.al., reported glutathione stimuli responsive PLGA based nanocarriers with for homoharringtonine delivery to lungs cancer with less side effect and improved therapeutic effects compared with free anticancer agents [37].

In the present study, we synthesized PLGA of M_w =13,900 by ring opening polymerization of D, L-lactide and Glycolide by green route with zinc proline initiator. The nanoformulation of LPs formulated with PLGA (M_n =13,900) as core material, DSPE/DSPE-PEG (2000) used for shell material and phospholipid S-100 molecular fence by nanoprecipitation method. The nanoformulation of LPs were characterized for different physicochemical and thermal properties. The cytotoxicity, cellular uptake and cell cycle analysis study of LPs performed in CT-26 cell lines. Biodistribution and tumor site retention was studied in CT-26 xenografts tumor bearing Balb/C mice. In-vivo tumor study in CT-26 injected Balb/C mice model proven better antitumor effect for P-DSPE-PEG-Ir. Overall study proven, P-DSPE-PEG-Ir LPs would be good nanoformulation for therapeutic delivery of Ir to colon cancer as alternatives to commercial Onivyde® Ir Pegylated liposomes approved by FDA. This LPs validated as a proof of concept to combat colon cancer.

2. Materials And Methods

2.1. Materials

DSPE and DSPE-PEG-2000 were obtained from Lipoid (Germany), D L-lactide and glycolide were purchased from Corbion Purac (Netherland),Ir obtained Generous gift from Emcure (Pune),1,1'-Dioctadecyl-3,3,3',3' Tetramethylindotricarbocyanine Iodide (DiR), 1,1'-Dioctadecyl-3,3,3',3'-Tetramethylindocarbocyanine Perchlorate-4' (DiI),6-Diamidino-2-phenylindole (DAPI), dialysis tubing (MWCO 2000 Da), SP-Sephadex C-25 resin were purchased from Sigma (UK). Snake Skin® dialysis tubing (MWCO 10000 Da) was a gift sample from Thermo-fisher (USA). Soybean lecithin (Epikuron 140 V) was a kind gift from Cargill Pharmaceuticals. Methylene chloride, acetone, n-hexane, absolute ethanol and diethyl ether (ultra-pure grades) were obtained from Sigma Aldrich (India). RPMI-1640 media,fetal bovine serum (FBS), penicillin/streptomycin, Trypsin/EDTA, and phosphate buffered saline (PBS) were obtained from Gibco, Invitrogen (India). BD flow cytometry tubes were purchased from VWR (UK). Vectashield®mounting media was from Vector Labs (UK); 16% Formaldehyde, methanol-free, was from Thermo Scientific Pierce. All reagents were used without further purification.

2.2 Synthesis of PLGA using ring opening polymerization

The ring opening polymerization of monomers of D, L-Lactide and Glycolide performed using Zinc proline complex [9]. Polymerization's reaction was carried out in bulk (without any solvent used in reaction medium) in sealed glass ampoules of (inner diameter of 2 cm and 10 cm in height). Glass ampoules were passivated using 20% TMSCl (Trimethyl silyl chloride in acetone solvent) before polymerization and dried properly in the oven. The addition of monomer and initiator was carried out in MBRAUN UNilab™ glove box to prevent moisture absorption in the monomers of D, L-Lactide and Glycolide. Ampoules were subjected to 3-4 Freeze-Pump-Thaw cycles in vacuo to remove moisture content from the monomers of D, L-Lactide and Glycolide. Ampoules containing D, L-lactide 50% mole (500 mg, 3.472 mmol), glycolide 50% mole (395 mg, 3.472 mmol) ratio initiator Zinc Proline (5 mg, 0.03472 mmol) respectively used to carry out polymerization reaction. The initiator zinc proline to monomer ratio 200 were used in the reaction sealed under vacuum. Ampoules were then immersed in Techne SBL-2D™ Fluidized sand bath previously

set at the temperature of 200 ˚C for 4h. Ampoules were cooled and broken so the solid material containing Poly (D, L-Lactide-co-Glycolide) polymer, and unreacted D, L-lactide, glycolide monomer was dissolved in a small amount of dichloromethane and precipitated in excess n-hexane to obtain a Poly (D, L-Lactide-co-Glycolide) polymer. Polymer samples were dried at 40 °C under vacuum for 48 h. Further characterized performed successfully. The polymerization reaction was reported with our research group in previous study for PLA repeated with some modification carried for PLGA [38].

2.3 Characterization of PLGA copolymer

The Synthesized PLGA copolymers were characterized by ^{1}H NMR, MALDI-TOF MS, Differential Scanning Calorimetry (DSC), Gel Permeation Chromatography (GPC) and ATR-FTIR etc.

2. 3.1 ^{1}H Nuclear magnetic resonance (NMR)

^{1}H-NMR spectra were recorded using 400 MHz Bruker 400 spectrometer using $CDCl_3$ as the solvent containing a small amount of the TMS as an internal standard. The sample preparation was carried out by dissolving 10 mg of PLGA polymers in $CDCl_3$ at room temperature.

2.3.2 Matrix assisted laser desorption ionization -Time of flight mass spectroscopy (MALDI-TOF MS)

MALDI-TOF MS analysis was performed on an AB SCIEX4800 plus MALDI TOF/TOFTM Analyzer. The PLGA copolymer samples were dissolved in tetrahydrofuran (1mg/mL) and mixed with the matrix (15mg/mL of tetrahydrofuran) and dried on the sample plate. 2,5-dihydroxybenzoic acid and dithranol were used as the matrix.

2.3.3 Differential scanning calorimetery (DSC)

Differential Scanning Calorimetry (DSC) measurements were performed on TA Instrument DSC Q10 in a nitrogen atmosphere. The heating rate was 10°C /min and cooling rate was 100°C/min for every run from 0°C to 200°C. The glass transition temperature data were recorded from second heating curves.

2.3.4 Gel permeation chromatography (GPC)

The molecular weights such as number-average molecular weight [Mn], weight-average molecular weight [Mw], and polydispersity [M_w/M_n] were determined with respect to polystyrene standards by size-exclusion chromatography on an Agilent Technologies, Polymer Laboratories Gel permeation chromatography (PL-GPC) 220 machine (Santa Clara, CA, USA) at 25 °C, with eluting PLGA solutions (10 mg/mL of $CHCl_3$) and toluene as an internal standard, and through a series of five 30 cm long Styragel columns with pore sizes of 500, 10^5, 10^4, 10^3, and 100Å. $CHCl_3$ was used as the mobile phase (flow rate: 1 mL/min), and a refractive index detector was used for the detection of different molecular weight fractions.

2.3.5 Attenuated total reflectance - fourier transform infrared (ATR-FTIR)

ATR-FTIR spectra of PLGA copolymer samples were recorded using a (Perkin Elmer IRFTIR spectrometer USA) in 500–4000 cm^{-2} wavelength range in attenuated total reflectance (ATR) mode. The instrument was calibrated with an indium standard before measurements.

2.4 Formulation of the LPs

LPs were formulated from PLGA, soybean lecithin with varied DSPE and DSPE–PEG-2000 shell using a modified nanoprecipitation technique [39]. PLGA was first dissolved in acetonitrile with concentration 1 mg/mL. Lecithin and DSPE/DSPE– PEG–2000 (7:3 molar ratio) were dissolved in 4% ethanol aqueous solution (aqueous phase) and 20 % of the PLGA (in acetonitrile as organic phase) weight with respect to lipid weight and heated to 65 ^{0}C temperature. The PLGA solution was then added slowly into the previously preheated lipid aqueous solution (DSPE/DSPE-PEG-2000 and Soyabean Lecithin) drop-wise (1 mL/min) under gentle stirring followed by vortexing for 3 min. The LPs were allowed to self-assemble for 2 h with continuous stirring while the organic solvent was allowed to evaporate. The remaining organic solvent and free molecules were removed by washing the LPs solution 3 times using an Amicon Ultra-4 centrifugal filter (Millipore, Billerica, MA) with a molecular weight cut-off of 10 kDa and then resuspended in water to obtain a final desired concentration. The LPs were freeze dried in liquid nitrogen and lyophilized for storage at -80 ^{0}C for later use [40-42]. P-DSPE-Ir LPs is referred to PLGA core, DSPE shell LPs loaded with Ir whereas P-DSPE-PEG-Ir LPs was referred to PLGA core DSPE-PEG_{2000} shell LPs loaded with Ir.

2.5 Characterization of the formulated LPs

Formulated nanoparticles were characterized for the following characterization as follows

2.5.1 Determination of percentage encapsulation efficiency

The encapsulation efficiency (EE %) of Ir loaded LPs was determined by measuring the concentration of the free drug in the LPs suspension. The unencapsulated Ir was separated by filtration followed by centrifugation. A definite volume of the LPs suspension was transferred to the upper chamber of the Nanosep and centrifuged at 6000 rpm for 60 min. The amount of free drug in the filtrate was measured using UV-vis spectrophotometer (Model UV- 1601 PC; Shimadzu, Kyoto, Japan) by measuring the absorbance at 360 nm as previously described [43-44]. The EE (%) was calculated by

EE (%) = ([Drug] total -[Drug] Supernatant)/[Drug] total) * 100

The percentage of drug loading efficiency (% LE) was calculated using the following equation:

LE (%) = Amount of Ir encapsulated (mg)/ weight of all excipients (polymer, Lipid and Soya lecithin) *100.

2.5.2 Size and Zeta potential measurements

The Polydispersity Index (PDI) and Zeta potential of LPs were determined by using zetasizer (PCS, Nano ZS90 zetasizer, Malvern Instruments Corp, U.K). Charge on the LPs surface was determined using zetasizer 300HSA (Malvern Instruments, Malvern, UK). Disposable polystyrene cells and disposable plain folded capillary Zeta cells were used. LPs suspensions were diluted in deionized water and measurements were performed at 25 °C. Electrophoretic mobility was used to calculate the zeta-potential using the Helmholtz-Smoluchowski equation. Analysis time was kept for 3 min and hydrodynamic size was presented as the average value of 20 runs, with triplicate measurements within each run.

2.5.3 Transmission Electron Microscopy (TEM)

Transmission electron microscopic (TEM) imaging of LPs was carried out using (FEI Technai G2 T20) instrument with an acceleration voltage of 200 keV. The TEM sample was prepared by transferring the LPs suspension (4 mg/mL) onto a 200-mesh carbon-coated copper grid. Samples were blotted away after 30 min incubation and grids were negatively stained for 10 min at room temperature with freshly prepared, 2% (w/v) phosphotungstic acid aqueous solution. The grids were then washed twice with distilled water and air-dried before imaging.

2.5.4 Atomic force microcopy (AFM)

The atomic force microscopy (AFM) measurements were performed on silicon wafer using a Multimode scanning probe microscope equipped with a Nanoscope IV controller from Veeco Instrument Inc., Santa Barbara, CA. All the AFM measurements were done under ambient conditions using the tapping-mode AFM probes model - Tap190Al purchased from Budget Sensors. The radii of tips used in this study were less than 10 nm, and their height was ~ 17 µm. The cantilever used had a resonant frequency of ca. 162 kHz and nominal spring constant of ca. 48 N/m with a 30 nm thick aluminium reflex coating on the back side of the cantilever of the length 225 µm. For each sample, three locations with a surface area of 1 × 1 µm2 and 500 × 500 nm^2, each were imaged at a rate of 1 Hz and at a resolution of 512× 512.

2.5.5 Wide angle X-ray Diffractometer (WAXD)

The lyophilized LPs were analyzed using wide angle X-ray Diffractometer (WAXD) in the range of 2θ=5-55° at room temperature (25 °C). The WXRD patterns of LPs sample were analyzed by Philips 1830 X-ray diffractometer (Philips, Almelo, The Netherlands) using a CuKα source at a (λ=1.5406 Å) to get more insights about nature of the sample.

2.6 In-vitro release profile

In vitro release from Ir loaded P-DSPE-Ir and P-DSPE-PEG-Ir LPs were determined by the previously reported dialysis method. 20 mg of LPs suspended in 10 ml of PBS buffer, was sealed in a dialysis bag (M.W. cut off: 10, 000, Sigma Aldrich). The dialysis bag was incubated in 100 ml of PBS buffer medium (pH 7.4 and 50% FBS in pH PBS) at 37 °C. The release amount was analyzed at 360 nm using Uv-visible spectroscopy Perkin-Elmer calculated using a calibration curve for Ir dissolved in the same media as the

dialysate (R^2 = 0.99995, range1-50 µg/mL) [45-46]. A control experiment was set up alongside in which the same amount of Ir was dissolved in DMSO and dialyzed for comparison. This control was set up to eliminate nonspecific adsorption of the drug to the dialysis membrane. The same conditions were used for P-DSPE-Ir and P-DSPE-PEG-Ir.

2.7 *In-vitro* anti-tumor efficacy studies

The I*n-vitro anti-tumor efficacy* of the blank P-DSPE, P-DSPE-PEG, P-DSPE-Ir and P-DSPE-PEG-Ir LPs was examined in CT-26 murine carcinoma cells by MTT assay. Cells were cultured (2×10^4 cells per well) in 96 well plate in RPMI media supplemented with 10% FBS, 1% penicillin, and 1% streptomycin in 5% CO_2 atmosphere at 37 °C. After 24 h incubation, different concentrations (5-100 µg/mL dispersed in media) of Ir, blank P-DSPE, P-DSPE-PEG, P-DSPE-Ir and P-DSPE-PEG- Ir LPs were added into wells. Following 24 hrs incubation, wells are washed with PBS, and 200 µL of MTT (0.5mg/ml) was added. Formazan crystals formed after 4 h were dissolved in 200 µL of DMSO. Optical absorbance was recorded at 570 using a microplate reader (Epoch2, BoiTek). The results were expressed as the percentage cell survival (mean ± SE) and calculated using the following equation:

% Cell survival = (A570 nm of treated cells/A570 nm of untreated control cells) x 100.

2.8 Fluorescence Labeling of LPs

Fluorescent labeled Dil and DiR dye loaded LPs were prepared for *In-vitro* uptake and *In -vivo* tumor targeting and biodistribution studies *In-vivo* imaging system (IVIS). Dil, emitting in the red region, and DiR, a fluorophore with near-infrared emission, are hydrophobic fluorescent markers that were incorporated into the organic phase at 0.5 % (w/v) (dye/organic phase) for *in vitro* and *in vivo* studies, respectively. Formulations were protected from light covered with aluminum foil and utilized for *in vitro* (P-DSPE-Dil and P-DSPE-PEG-Dil) and *in vivo* (P-DSPE-DiR and P-DSPE-PEG-DiR) studies.

2.9 Cellular uptake

CT-26 cells were seeded on coverslips at a density of 1×10^5 cells /well. To check the uptake efficiency of nanoparticles, cells were treated with Dil tagged LPs (P-DSPE-Dil and P-DSPE-PEG-Dil). After 4 hrs, media containing nanoparticles were removed and cells were fixed with 4% paraformaldehyde for 20 min. The coverslips, were mounted onto slides and uptake was visualized using Leica sp5 confocal microscope. In separate experiments, cells were treated with cold temp (4^0C) or sodium azide (0.1%) or sucrose (0.5M) or amphotericin B (20mM) for 1hr as inhibitor of uptake pathways prior to treatment with LPs followed by confocal analysis.

2.10 Cell cycle analysis

Effect of Ir loaded P-DSPE-Ir and P-DSPE-PEG-Ir LPs on cell cycle progression in CT-26 cells was analyzed by FACS. Briefly, CT-26 cells were seeded in a 60 mm dish at a density of 2×10^5 cells /dish and treated

with NPs (50 µg/ml) for 24 h. After treatment, cells were fixed overnight in 95% ethanol at 4^0C and were washed in chilled PBS for 2 times, the pellet was re-suspended in 50 µl of RNase A (0.5 mg/ml) and incubated for 20 minutes at 37 °C. After that, 450 µl of propidium iodide (50µg/ml) was added. The proportion of cells at different phases of the cell cycle was monitored by FACS Calibur (BD Biosciences).

2.11 In-vivo Biodistribution study

All animal procedures were performed in accordance with the Guidelines approved by 'Committee for the Purpose of Control and Supervision of Experiments on Animals' (CPCSEA), Government of India and experiments were approved by Institutional Animal Care and Use Committee (IACUC) of National Centre for Cell Science (NCCS), Pune, India.6–8 week's old female Balb/C mice were used to perform the *in vivo* studies. CT-26 colon cancer cells (1×10^6) mixed with Matrigel were injected subcutaneously into the right flanke of mouse, and tumor growth was observed. After tumor generation, DiR loaded P-DSPE-DiR and P-DSPE-PEG-DiR loaded LPs were injected intravaneously through tail vein of the mice. The biodistribution of DiR loaded nanoparticles monitored at various time points upto 7 days by *In-vivo* imaging. The biodistribution of the DiR in major organs (heart, lung, liver, spleen, intestine, and kidney) and tumor was examined by e*x-vivo imaging* after sacrifice of mice using the IVIS system (IVIS spectrum, Xenogen). In separate experiments, CT-26 tumor bearing mice were injected with (P-DSPE-DiL and P-DSPE-PEG-DiL) and tumor retention of NPs was analyzed for 9 days using IVIS.

2.12 In-vivo anti-tumor efficacy studies

All animal procedures were performed in accordance with the Guidelines approved by 'Committee for the Purpose of Control and Supervision of Experiments on Animals' (CPCSEA), Government of India and experiments were approved by Institutional Animal Care and Use Committee (IACUC) of National Centre for Cell Science (NCCS), Pune, India.CT-26 colon cancer cells (1×10^6) mixed with Matrigel were injected subcutaneously into the right flanke of mouse, and tumor growth was observed. After tumor initiation, mice were treated with Ir, P-DSPE-Ir and P-DSPE-PEG-Ir nanoparticles (10 mg/kg body wt Ir corresponding conc.) intravenous twice a week for two weeks. The tumor size monitored with the help of Vernier caliper during the experiment. After two weeks, mice were sacrificed, tumors were harvested and weighed. Further, tumors sections were prepared for histopathological analysis.

2.13 In-vivo acute toxicity studies

All animal procedures were performed in accordance with the Guidelines approved by 'Committee for the Purpose of Control and Supervision of Experiments on Animals' (CPCSEA),Government of India and experiments were approved by Institutional Animal Care and Use Committee (IACUC) of National Centre for Cell Science (NCCS), Pune, India.6-8 week old healthy female Balb/c mice were treated with Ir, P-DSPE-Ir and P-DSPE-PEG-Ir LPs (20 mg/kg body wt of Ir corresponding conc) twice a week for two weeks. After one week, blood was drawn from mice through retro-orbital sinus and hematological and biochemical analysis was performed to examine the toxicity.

2.14 Stastical analysis

For all experiments, data were presented as mean ± SD. Significant differences were examined using one-way ANOVA. $p<0.05$ was considered statistically significant in all studies.

3. Results

3.1 Synthesis of PLGA copolymer

3.1.1 Ring opening polymerization of D, L-lactide and Glycolide

PLGA was synthesized by using ring opening polymerization of D, L-lactide and glycolide in presence of zinc proline complex as shown in (Scheme 1). The molar ratios of D, L-lactide and glycolide (50:50) were used. Reaction conditions such as polymerization temperature (200 °C), monomer to initiator ratio ([M]/[I]= 200) and reaction time (4hr) were maintained. The molecular weight was obtained of M^w=13,900 and Polydispersity Index PDI=1.7 which indicates as narrow molecular weight distribution. This polymer further used for formulation of Ir loaded LPs.

3.2 Characterization of copolymer

The characterization of the synthesized PLGA copolymer performed by different technics like ATR-FTIR,^{1}H-NMR, *^{1}H-NMR* and Molecular weight determination by GPC which are described.

3.2.1 Attenuated total reflection- Fourier-transform infrared' spectroscopy

ATR-FTIR spectrum of PLGA polymer presented in (Fig.S1). The FTIR spectrum of PLGA shows peak at 1740 cm^{-1} (ester C=O stretching) and at 1065 cm^{-1} (O-CH_2 stretching). The peaks appear at 3500 cm^{-1} (O-H stretching) belong to the terminal hydroxyl groups in the copolymer is weak. The absorptions at the range 2900-3000 cm^{-1} represent C-H stretching of -CH- and CH_2 groups, respectively. These all peaks are according to results reported in the literature for PLGA.

3.2.2 ^{1}H-NMR

^{1}H NMR spectrum of PLGA copolymer as shown in (Fig.1). The methine (CH) and methyl (CH_3) of lactide protons appear at 5.2 ppm and 1.52 ppm. The CH_2 of glycolide appears at 4.8 which confirmed the structure of PLGA.

3.2.3 Molecular weight determination by GPC

The weight average molecular weight (M_W) was determined by GPC reported 13,900 Da with narrow polydispersity index (PDI=1.7). The SEC chromatograph is shown in **(Fig.2).** The PDI reported is significantly good as compared with obtained from polymerization reactions with Stannous octoate based catalyst.

3.3. Formulation and physico-chemical characterization of LPs

The formulation of P-DSPE-Ir LPs performed as initially PLGA (M_w=13,900 Da) dissolved in acetonitrile (1mg/mL of M=13,900 PLGA) and lipid/DSPE molar ratio (9:1) were used for optimized batch of LPs schematic presentation is as showed in the (Scheme 2). These formulated LPs showed aggregation above 2 um size. This result attributed to improper coverage of PLGA core by phosphatidylcholine layer. Then, the effect of lipid/DSPE molar ratio on the size of LPs was studied. We varied the lipid/DSPE molar mass ratios of 9:1, 8:2,7.5:2.5 or 7:3, whereas total lipid/polymer mass ratio of 10%, 15% or 20% are depicted in (Table S1 and Fig.S2). Aggregations were observed with 9:1 molar ratio, an increase in the lipid/DSPE, therefore, we have selected formulations (P_7) because the diameters were less than 100 nm. Similarly, the study of lipid/polymer mass ratio and DSPE/lipid molar ratio formulation parameters were optimized for LPs with low nm diameter. Hence, optimized LPs formulation was sufficient for 10% of lipid/polymer mass ratio and 7.5:2.5 lipid/DSPE molar ratio to form total lipid coverage so that the PLGA hydrophobic core with nanometer range. Similarly, optimization was carried for the P-DSPE-PEG LPs where optimization for batch (P8) showed less particle size as shown in (**Table S2 and Fig.S3**) for optimization of the formulation. The physicochemical properties of the optimized formulation are shown in (**Table 1**).

Table 1. Physicochemical Characterization of PLGA Based LPs

Formulation [a]	Day	Hydrodynamic diameter (nm)[b,f]	Polydispersity index[b,f]	Zeta-Potential (mV) [c,f]	Encapsulation Efficiency (EE%)[d,f]	Loading Efficiency (LE%) [d,f]
P-DSPE–Ir (P7)	0	118±9	0.300±0.04	-38±4.6	75.5±6.0	15.5±3.3
	7	125±5	0.312±0.03	-37.76±5.4		
	28	131±6.5	0.315±0.02	-36.42±3.4		
P-DEPE-PEG-Ir (P8)	0	77±3.2	0.232±0.03	-37.5±1.6	85±2.0	17.5 ±3.8
	7	81±4.8	0.258±0.01	-37±4.2		
	28	95±6.1	0.279±0.04	-36±3.1		

[a]Ir 5 mg, PLGA, Soya lecithin, DSPE/DSPE or DSPE-PEG_{2000} as per molar ratio

[b] Measured by dynamic light scattering.

[c]Surface charge measured by electrophoresis.

[d] Calculated as a percentage of initial drug added, determined by spectrophotometry.

[e] Calculated as a mass of incorporated drug divided by the weight of the polymer, determined by spectrophotometry.

[f] Expressed as mean ± SD (n=3).

3.4 Transmission electron microscopy (TEM)

Transmission electron microscopy (TEM) was, used to observe the inner structure and the morphological characteristics of the LPs formulated in this work. This method allows the measurement of the size of the LPs in a partially dried state. The average diameters were found to be 40-50 nm for P-DSPE-Ir and P-DSPE-PEG-Ir LPs and core-shell morphology is shown in (Fig.3 a-b).

3.5 Atomic force microscopy (AFM)

Atomic force microscopy images of nanoparticles are as shown in (Fig.4a-b), which again confirm spherical morphology of nanoparticles with uniform distribution of spherical LPs**.** AFM confirm 3 dimensional morphology of LPs.

3.6 Wide angle X-ray diffraction analysis

Wide angle X-ray diffraction analysis of all excipients and LPs as shown in **(Fig.5).** Ir shows sharp crystalline peaks in the range of diffraction angle from 2θ = 7-25°. DSPE and DSPE- PEG lipids showed crystalline diffraction discontinuous peaks in the range of diffraction angle from 2θ = 8-40°. DSPE and DSPE-PEG containing PLGA LPs showed lesser intensity of diffraction peaks which are attributed to DSPE and PEG segment of LPs and absence of the characteristic peaks of observed for Ir. Absence of Ir diffraction, peaks confirmed its uniform distribution in LPs. WAXD pattern of LPs (P-DSPE-Ir and P-DSPE-PEG-Ir) showed an amorphous nature as compared to pure Ir

3.7 Differential scanning calorimeter

The thermal analysis of Ir, PLGA, DSPE, DSPE-PEG and P-DSPE-Ir/P-DSPE-PEG-Ir LPs are shown in **(Fig.6).** DSC curve showed the melting point (T_m) of Ir at 245 °C indicating crystalline nature. PLGA showed the glass transition temperature (T_g) at 30.8 °C which can be attributed to amorphous nature of polymeric chain. DSPE lipid showed a melting point (T_m) of 99 °C and DSPE-PEG-2000 showed a melting point (T_m) of 39 °C due to its crystalline nature. Ir not showed any transition in the curve which is indicative of uniform dispersion of LPs of P-DSPE-Ir. In case of P-DSPE-PEG-Ir LPs showed T_m at 30.1°C which is attributed to the PEG segment of the DSPE-PEG. Absence of Ir melting point (T_m) in both LPs indicated the amorphous phase transformation for Ir and uniform distribution in polymer lipid matrix.

3.8 Drug release studies

It was observed that the two formulations: P-DSPE-Ir and P-DSPE-PEG-Ir exhibited similar release profiles (10-15 % drug release observed) in the presence or absence of serum up to 1 h without initial burst release **(Fig. 7a-b).** In the absence of serum, a total of 60-70% of the drug was released over the first 24 h with no significant differences between the two formulations. In the presence of serum, approximately 70 % of the drug was released over 24 h there was no significant difference between the two formulations. On the other hand, DMSO control showed the rapid release of the drug into the dialysate with more than 95% of the drug was released within the 24 h, as expected. These LPs showed In line study showed minimized burst release which is major drawback of the polymeric nanoparticles. The formulated LPs showed sustained release for 84 hr. This lipid polymer matrix is not pH responsive, for same reason release at weak acidic tumor conditions are not performed.

3.9 In-vitro Cytotoxicity studies in CT- 26 cell

MTT assay was used to study the *In vitro* cytotoxicity of the Ir, blank and Ir loaded P-DSPE-Ir and P-DSPE-PEG LPs in CT-26 murine colon carcinoma. Cells were incubated with all treatment of drug concentrations (5-100 µg/ml) for 48 h. Blank DSPE, blank DSPE-PEG LPs were found to be nontoxic for cells after 48 h as shown in whereas P-DSPE-Ir and P-DSPE-PEG-Ir LPs shown concentration dependent cytotoxicity (**Fig.8**). Ir loaded LPs showed statistically improved cell toxicity in higher extent compared with similar concentration of Ir. The difference in the IC_{50} values was obtained for P-DSPE-Ir and P-DSPE-PEG-Ir LPs which resulted in differences in cytotoxicity. A similar trend was observed at the highest concentration tested (100 µg/ml). The CT-26 cell lines were found to be more sensitive to P-DSPE-PEG-Ir as compared to P-DSPE-Ir LPs as PEG layer responsible for fate of LPs In-vitro.

3.10 Cellular uptake study of P-DSPE-PEG LPs

Cellular uptake of LPs confirmed with confocal laser scanning microscopy (CLSM) as shown in (Fig.9a). To confirm intracellular delivery of the LPs loaded with Dil dye, CT-26 cells were treated with P-DSPE and P-DSPE-PEG loaded Dil dye used in fluorescence measurements. Cells were fixed and examined by CLSM. The uptake of the LPs was confirmed by the presence of red signals as shown in (Fig.9b). The results confirmed the enhanced cellular uptake of P-DSPE-DiL in CT-26 cells which confirmed significant higher uptake where as P-DSPE-PEG-Dil LPs indicated lower intensity of signal in the CLMS measurement both qualitatively and quantitatively. Due to presence of PEG layer on the surface of P-DSPE-PEG-Ir LPs showed decreased cellular uptake compared to P-DSPE-Ir LPs due to PEG layer cause hydration and cytomembrane is a lipid soluble membrane. The enhanced uptake of P-DSPE- Dil LPs was obtained as compared to P-DSPE-PEG-Dil. Cellular uptake using confocal laser scanning microscopy (CLSM) image showed in the (Fig.9c). CT-26 cells were treated with P-DSPE-PEG loaded with Dil dye kept at 4 °C or again retreated with cell uptake inhibitors (37 °C) such as sodium azide, and Nystatin. It has observed that no apparent fluorescence was observed in the CT-26 cells kept at 4 °C, and sucrose shown fluroscence for DiL labelled LPs indicates active transport, and passive transport are not cellular uptake pathway for these LPs. Furthermore, no fluorescence intensity was observed in the cells treated with sodium azide and

Nystatin indicates clathrin as well as caveole medicated cellular uptake are major pathway for uptake into CT-26 cells .

3.3.11 Cell cycle analysis

The cell cycle analysis results for control, Ir and Ir loaded LPs as shown in (Fig.10 a-b). The results suggested that Ir and Ir loaded LPs, induced cell cycle arrest in the G2M phase of cell cycle which might be the reason for subsequent apoptosis. However, Ir loaded P-DSPE-Ir, P-DSPE-PEG-Ir LPs induced higher cell death by the increase in sub G0 population in the treated cells. Sub G0 population represented the dead cell population. Hence, the increase in the Sub G0 population indicated the induction of cell death.

3.3.12 In-vivo biodistribution study

In-vivo biodistribution of P-DSPE and P-DSPE-PEG loaded DiR LPs nanocarrier's observed in CT-26 colon tumor xenograft models. Whole body imaging was carried out up to 72 h after Intravenous tail injection followed by *ex-vivo* imaging of excised tissues. Tumor uptake of P-DSPE and P-DSPE-PEG was observed in both tumor xenografts when imaged from the dorsal view showed intensity of DiR loaded LPs shows in (**Fig.11a**). In contrast to these treatment control mice injected blank LPs, no fluorescence signals were detected from control mice. The fluorescence image of excised organs is showed in (**Fig.11b**), where the highest fluorescence intensities were measured from the liver, tumor and followed by spleen. Fluorescence intensities from each organ were further quantified and results were showed in (**Fig.11c**). Taking into account, weights of the samples, slightly higher fluorescence signals per gram of tissue calculated from the liver, lung than tumors. Lower values were obtained from the rest of the tissues which was expected from the fluorescence image as shown in (**Fig. 11b**). The comparison of fluorescence intensity from the graphs showed that where P-DSPE-PEG-DiR loaded dye LPs appeared more intense as compared to P-DSPE-DiR loaded dye LPs. *In vivo* tumor site retention of DSPE-PEG LPs showed better fluorescence intensity as compared with P-DSPE LPs shown in (Fig.S4). These LPs showed sufficient retention at tumor site; therefore, can be used in diagnostic applications

3.3.13 Delay tumor growth study

Mice bearing subcutaneous CT-26 inoculated tumors of 50-70 mm^3 were treated with 10 mg/kg of Ir or Ir equivalent LPs of P-DSPE-Ir and P-DSPE-PEG-Ir by Intravenous at tumor site twice a week for two weeks and tumor size was measured with venire caliper as showed in the (**Fig.12.a-b**). The P-DSPE-Ir and P-DSPE-PEG-Ir LPs shown statistically significant delay in the tumor growth. Similarly, body weight measurement was carried out on same day of tumor size analysis. After sacrifice on 12 days tumor weight analysis performed which indicates Ir in LPs showed less tumor weight as compared with Ir and Control treatment group indicated in the (**Fig.12c**). The H&E staining was further confirmed the absence of observable organ toxicity. P-DSPE-PEG-Ir shows better results as compared with P-DSPE-Ir due lower immunogenicity, shielding of LPs from opsonization, phagocytosis, aggregation and prolonged circulation. Histopathological analysis of mice organ for different treatment after completion of therapy

shown in the (Fig.12d). Histopathological analysis proven non abnormality in the all organs stained with (E and H) which indicates biocompatibility and safety of nanoformulations.

3.3.15 In-vivo toxicity study

Acute toxicity of Ir, Phosphate buffer solution (PBS), P-DSPE-Ir and P-DSPE-PEG-Ir LPs (equivalent of Ir doses (20 mg/kg) of four doses were administrated by Intravenous twice week in the Balb/C mice to check toxicity of the nanocarrier. The body weight and food intake were recorded every two consecutive days. The biochemical and blood routine examination were tested after Day 14 th day and histopathological evaluation was carried out to confirm the major organs toxicity. The results of the toxicity study confirm no significant difference except hematological analysis proven neutropenia side effect associated with Ir was not reported for P-DSPE-Ir and P-DSPE-PEG-Ir LPs as shown in the (**Fig.13 a-e)**. Neutropenia is major side effect of Ir reported in the patient undergoing chemotherapy. Ir in the form of P-DSPE-Ir and P-DSPE-PEG-Ir LPs cause significant delay in the neutropenia which is beneficial for patient undergoing chemotherapy with Ir.The Hematological and biochemical parameters are shown in (**Table. S3 and Fig.14)** respectively. Histopathological analysis confirms no sign of toxicity as shown in the **(Fig.15)** and hence, these LPs proven its safety in present study for future chemotherapy application.

4. Conclusion

Synthesis PLGA copolymer performed by green route using zinc proline initiator by ring-opening polymerization reaction to avoid non-toxic biocompatible excipient. This polymer well characterized by GPC,1H and thermal analysis. This polymer used for formulation of Ir loaded P-DSPE-Ir, P-DSPE-PEG-Ir LPs were formulated by nanoprecipitation method and LPs well characterized using dynamic light scattering for particle size analysis/zeta potential, morphological characterization performs with transmission electron microscopy. Differential scanning calorimetry and X-ray diffraction analysis reveals amorphous transformation of crystalline Ir in LPs. Further, Ir release study carried out in PBS pH 7.4 buffer and 50% FBS showed the sustained release of P-DSPE-Ir and P-DSPE-PEG-Ir without significant difference between the release pattern. However, no burst release was observed for LPs which is major issue with polymeric nanoparticles. Stability study carried out up to 28 days at 4˚C, confirmed the stability of these formulations with no change in particle size and zeta potential observed. Entrapment efficiency for P-DSPE-PEG-Ir is higher as compared to P-DSPE-PEG-Ir LPs.This contributes to higher efficiency and therapeutic effect *In-vivo*. The cytotoxicity assay of LPs in CT-26 cells shown P-DSPE-PEG-Ir LPs are more sensitive as compared to DSPE-Ir LPs. Confocal microscopy confirmed greater uptake and cellular internalization of P-DSPE-PEG Dil loaded LPs as compared to P-DSPE Dil loaded LPs.These LPs uptake into cell via clathrin and caveole mediated uptake. The biodistribution study of DiR loaded P-DSPE and P-DSPE-PEG LPs carried *in-vivo* and *ex-vivo* proven better tumor accumulation in CT-26 inoculated mice. The *In-vivo* anticancer activity of Ir loaded LPs showed better delay in tumor growth for P-DSPE-PEG-Ir treatment group as compared with Ir, P-DSPE-Ir and control group. The acute toxicity study of these LPs showed biocompatible and nontoxic nature of LPs. The neutropenia side effect of Ir significantly reduced in Ir encapsulated P-DSPE-Ir/P-DSPE-PEG-Ir nanocarriers. In the literature our previous study

report m-PEG-PLGA based nanoparticles with Tween-80 and Pluronics coating successfully used for pancreatic, colon cancer delivery-PEG-PLGA based nanoparticles shown better tumor growth delay and non-immunogenicity, biocompatibility [47]. In the present study Overall results, reported synthesis of PLGA and theire characterization and further well characterized for colonic delivery applications. *In-vitro* and *In-vivo* study confirm P-DSPE-PEG-Ir perform better as compared with P-DSPE-Ir due to prolonged circulation, decrease immunogenicity, less agrregation, opsonization results into prolong circulation to combat colon cancer. The results obtained shows desired properties for used in the drug delivery application. Ir in the PLGA based LPs nanocarrier improved safety, efficacy, bioavailability for efficient delivery to colon cancer.

Declarations

Ethics approval and consent to participate: (Not Applicable)

Consent for publication: All author given consent for publication of manuscript

Availability of data and materials: (Not Applicable)

Competing interests: All author has non-conflict of interest

Funding: (Not Applicable)

Authors' contributions: Dr. Prabhanjan Giram performed all work along with Dr. Baijayntimala Garnaik

Acknowledgements: The authors are thankful for UGC for fellowship, CSIR-NCL and NCCS for facility and infrastructure for research work.

Authors' information (optional): (Not Applicable)

References

1. Haitao Q, Adam RW, Jordan TC, Christopher WM, Thomas RH. A Strategy for Control of “Random” Copolymerization of Lactide and Glycolide: Application to Synthesis of PEG-b-PLGA Block Polymers Having Narrow Dispersity. Macromolecules. 2011; https://doi.org/ 10.1021/ma201169z.
2. Analı´a S, Alicia GC, Mercedes V, Analı´a R, Santiago DP, Jose´ M, editors. Nanotechnology applications in drug controlled release Drug Targeting and Stimuli Sensitive Drug Delivery Systems. Elsevier; 2018. pp. 1–116.
3. Moghimi SM, Hunter AC, Murray JC. Long-circulating and target-specific LPs: theory to practice. Pharmacol Rev. 2001. pp.283–318.
4. Sophia V, Melissa F, Etienne V. Cognitive Training for Impaired Neural Systems in Neuropsychiatric Illness. Neuropsychopharmacology. 2012.pp.43–76.

5. Ronnie HF. Santosh A. Che-Ming J. Liangfang Z. Quick Synthesis of Lipid – Polymer Hybrid Nanoparticles with Low Polydispersity Using a Single-Step Sonication Method. Langmuir.2010; https://doi.org/ 10.1021/la103576a.
6. Cheow WS. Kunn H. Factors affecting drug encapsulation and stability of lipid-polymer hybrid nanoparticles. Colloids Surf B Biointerfaces. 2011; https://doi.org/ 10.1016/j.colsurfb.2011.02.033.
7. Maurer N. Fenske DB. Cullis PR. Developments in liposomal drug delivery systems. Expert Opin Biol Ther 2001; https://doi.org/ 10.1517/14712598.1.6.923.
8. Robson F, John WS. Kinetics and Mechanism of the Stannous Octoate-Catalyzed Bulk Polymerization of ε-Caprolactone. Macromolecules; 2002. https://doi.org/10.1021/ma010986c.
9. Akhilesh KM. Anamika M. Nidhi M. Nanoengineered polymeric biomaterials for drug delivery system. Woodhead Publishing Series in Biomaterials.2020;https://doi.org/10.1016/B978-0-08-102985-5.00006-1.
10. Nikalje PG. Nanotechnology and its Applications in Medicine.2015; https://doi.org/10.4172/2161-0444.1000247.
11. Xiaorong W. James EH. Sandra W. James K. Jeffery MM. Mindaugas R. Georg GA. Synthesis, Characterization, and Application of Novel Polymeric Nanoparticles.Macromolecules.2007; https://doi.org/ 10.1021/ma0613739.
12. Anil K. Fei C. Anbu M. Xu Z. Yuanyuan Z. Xiangdong X. Yanli H. Xiaoning Z. Paul C, Xing-Jie L. Innovative pharmaceutical development based on unique properties of nanoscale delivery formulation. Nanoscale. 2013; https://doi.org/ 10.1039/c3nr01525d.
13. Eleni G. Konstantinos A. Milan P. Miroslav P. Dimitrios P. Halloysite nanotubes as carriers for Ir: Synthesis and characterization by experimental and molecular simulation methods. Journal of Drug Delivery Science Technology. 2019. https://doi.org/10.1016/j.jddst.2019.05.001.
14. Teresa DD. Alessandro A. Paola O. Silvia MF. Anna F. Greta A. Gabriella F. Fulvio B. Giulio F. Guido B. Synergistic efficacy of Ir and sunitinib combination in preclinical models of anaplastic thyroid cancer. Cancer Lett. 2017. doi. 10.1016/j.canlet.2017.09.032.
15. Padma VD. Anil BJ.Rajesh RP. Particle Shape: A New Design Parameter for Passive Targeting in Splenotropic Drug Delivery. J Pharm Sci. 2010. doi:10.1002/jps.22052.
16. Ki YC. Eun JJ. Hong YY. Beom SL. Jin HNa. Kyung HM. Sang YK. Seung-Jae M. Theranostic LPs based on PEGylated hyaluronic acid for the diagnosis, therapy and monitoring of colon cancer. Biomaterials. 2012. https://doi:10.1016/j.biomaterials.
17. Verreault M, Strutt D. Masin D. Anantha M. Waterhouse D. Yapp DT. Bally MB. Irinophore C™, a lipid-based nanoparticulate formulation of Ir, is more effective than free Ir when used to treat an orthotopic glioblastoma model. J Controlled Release. 2012. https://doi.org/10.1016/j.jconrel.2011.09.095.
18. Liu J. Chi D. Pan S. Zhao L. Wang X. Wang D. Wang Y. Effective co-encapsulation of doxorubicin and Ir for synergistic therapy using liposomes prepared with triethylammonium sucrose octasulfate as

drug trapping agent International. Journal of Pharmaceutics. 2019. https://doi:10.1016/j.ijpharm.2018.12.072.

19. Einafshar E. Asl AH. Nia AH. Mohammadi M. Malekzadeh A. Ramezani M. New cyclodextrin-based nanocarriers for drug delivery and phototherapy using an Ir metabolite. Carbohyd Polym. 2018. doi. 10.1016/j.carbpol.2018.03.102.
20. Chang J. Rodriguez-Bigas MA. Skibber JM. Moyer VA. Lymph node evaluation and survival after curative resection of colon cancer: systematic review. J Natl Cancer Inst. 2007. doi. 10.1093/jnci/djk092.
21. Ankit S, Robin K, Mubashir JM. Ravindra DD. Payare LS. Dilip MM. Amulya KP. Prem NG. Gemcitabine and betulinic acid co-encapsulated PLGA – PEG polymer nanoparticles for improved efficacy of cancer chemotherapy. Materials Science Engineering: C. 2019. doi. 10.1016/j.msec.2019.01.026.
22. Danjun Wu. Lixi Zhu. YiLi Hui. ying Wang. Shumin Xu. Xueling Zhang. Rui Wu. Gensheng Yang. Superparamagnetic chitosan nanocomplexes for colorectal tumor-targeted delivery of Ir. International Journal of Pharmaceutics.2020; https://doi:10.1016/j.ijpharm.2020.119394.
23. England RM. Hare JI. Barnes J. Wilson J. Smith A. Strittmatter N. Kemmitt PD. Waring MJ. Barry ST. Alexander C. Ashford MB. Tumour regression and improved gastrointestinal tolerability from controlled release of SN-38 from novelpolyoxazoline-modifieddendrimers. J Controlled Release. 2017. https://doi.org/10.1016/j.jconrel.2016.12.034.
24. Gao YE. Bai S. Shi X. Hou M. Ma X. Zhang T. Xiao B. Xue P. Kang Y. Xu Z. Ir delivery by unimolecular micelles composed of reduction-responsive star-like polymeric prodrug with high drug loading for enhanced cancer therapy. Colloids Surf B. 2018. doi. 10.1016/j.colsurfb.2018.06.054.
25. Wang L, Liu X. Zhou Q. Sui M. Lu Z, Zhou Z, Tang J, Miao Y, Zheng M, Wang W, Shen Y. Terminating the criminal collaboration in pancreatic cancer: Nanoparticle-based synergistic therapy for overcoming fibroblast-induced drug resistance. Biomaterials. 2017. doi. 10.1016/j.biomaterials.2017.08.002.
26. Monterrubio C. Pascual-Pasto G. Cano F. Vila-Ubach M, Manzanares A. Schaiquevich P. Tornero JA. Sosnik A. Mora J. Carcaboso AM. SN-38-loaded nanofiber matrices for local control of pediatric solid tumors after subtotal resection surgery. Biomaterials. 2016. https://doi.org/10.1016/j.biomaterials.2015.11.055.
27. Shire Z, Vakili MR, Morgan TD, R, Hall DG, Lavasanifar A, Weinfeld M. Nanoencapsulation of Novel Inhibitors of PNKP for Selective Sensitization to Ionizing Radiation and Ir and Induction of Synthetic Lethality. Mol Pharmaceutics 2018; https://doi.org/doi: 10.1021/acs.molpharmaceut.8b00169.
28. Bethesda MD, FDA approves new treatment for advanced pancreatic cancer U.S. Food and Drug Administration American Cancer Society. Cancer facts & figures. 2015.
29. Wagner D, Kern WV, Kern P. Liposomal doxorubicin in AIDS-related Kaposi's sarcoma: long-term experiences. Clin Investigation. 1994. doi:10.1007/BF00180514.

30. Bogner JR. Kronawitter U. Rolinski B. Truebenbach K. Goebel FD. Liposomal doxorubicin in the treatment of advanced AIDS-related Kaposi sarcoma. J Acquir Immune Defic Syndr. 1994; pp. 463–8.
31. Gottlieb JJ. Washenik K. Chachoua A. Friedman-Kien A. Treatment of classic Kaposi's sarcoma with liposomal encapsulated doxorubicin. Lancet 1997; https:// doi:10.1016/S0140-6736(05)65133-1.
32. Phatsapong Y.Danuta SK. Des RR. Lipid-Based Drug Delivery Systems in Cancer Therapy. Pharmacol Rev 2016; https:// doi:10.1124/pr.115.012070.
33. Mandal B. Mittal NK. Balabathula P. Thoma LA. Wood GC. Development and in vitro evaluation of core-shell type lipid-polymer hybrid LPs for the delivery of erlotinib in non-small cell lung cancer. Eur J Pharm Sci. 2016. doi. 10.1016/j.ejps.2015.10.021.
34. Mori THazekawaM, Yoshida M. Nishinakagawa T. Uchida T. Ishibashi D. Enhancing the anticancer efficacy of a LL-37 peptide fragment analog using peptide-linked PLGA conjugate micelles in tumor cells. Int J Pharm. 2021 Sep;5:606:120891.
35. Samadzadeh S, Mousazadeh H, Ghareghomi S, Dadashpour M, Babazadeh M, Zarghami N. In vitro anticancer efficacy of Metformin-loaded PLGA nanofibers towards the post-surgical therapy of lung cancer. Journal of Drug Delivery Science and Technology. 2021 Feb 1;61:102318.
36. Wang Z, Chui WK, Ho PC. Design of a multifunctional PLGA nanoparticulate drug delivery system: evaluation of its physicochemical properties and anticancer activity to malignant cancer cells. Pharmaceutical research. 2009 May;26(5):1162–71.
37. Zhang Z, Cheng W, Pan Y, Jia L. An anticancer agent-loaded PLGA nanomedicine with glutathione-response and targeted delivery for the treatment of lung cancer. Journal of Materials Chemistry B. 2020;8(4):655–65.
38. Sharad PP. Shrikant DW. Manoj VM. Pranita SS. Baijayantimala G. Investigation of the biocompatibility and cytotoxicity associated with ROP initiator and its role in bulk polymerization of l-lactide. Polymer. 2017. https://doi.org/10.1016/j.polymer.2017.01.058.
39. Chan JM. Zhang L.Yuet KP. Liao G. Rhee JW. Langer R. Farokhzad OC. PLGA-lecithin-PEG core-shell LPs for controlled drug delivery. Biomaterials. 2009. doi. 10.1016/j.biomaterials.2008.12.013.
40. Ping H. Minxi Hu. Linzhu Z. Yao W. Yan P. Gangsheng T. Wei H. Xinyuan Z. **Polymeric Nanoparticles with Precise Ratiometric Control over Drug Loading for Combination Therapy**. RSC Adv. 2015; https://doi.org/10.1021/mp200243k
41. Kumaresh S, Soppimatha S, Tejraj M. A. Biodegradable polymeric nanoparticles as drug delivery devices. J Controlled Release. 2001. https://doi.org/10.1016/S0168-3659.
42. Wim HDe, Paul JA. Drug delivery and nanoparticles: Applications and hazards. Int J Nanomedicine. 2008. doi:10.2147/ijn.s596.
43. Sharma S. Sharma MC. Development and validation of Spectrophotometric method and TLC Densitometric Determination of Ir HCl in pharmaceutical dosage forms. Arabian Journal of Chemistry. 2010. https://doi.org/10.1016/j.arabjc.2012.02.012.
44. Eri AT. Folarin EL. Microfluidic Synthesis of Lipid-Polymer Hybrid Nanoparticles for Targeted Drug Delivery. MRS Advances. 2016. https://doi.org/10.1063/1.4922957.

45. Qiwen Z. Bin B. Qiumeng Z. Jiahui Y. Wei, Lu. Maleimidation of dextran and the application in designing a dextran–camptothecin conjugate. RSC Adv. 2018. https://doi.org/10.1039/C7RA12954H.
46. Bernhard I. Stefan W. Hanna E. Liposome-Coated Iron Fumarate Metal-Organic Framework Nanoparticles for Combination Therapy. Nanomaterials 2017 https://doi.org/10.3390/nano7110351.
47. Giram P, Wang J, Walters A, Rade P, Akhtar M, Han S, Faruqu F, Abdel-Bar H, Garnaik B, Al-Jamal K. .Green synthesis of methoxy-poly(ethylene glycol)-block-poly(l-lactide-co-glycolide) copolymer using zinc proline as a biocompatible initiator for Ir delivery to colon cancer in vivo. Biomater Sci. 2021; https://doi.org/ 10.1039/D0BM01421D.

Scheme

Schemes 1 and 2 are available in the Supplemental Files section

Figures

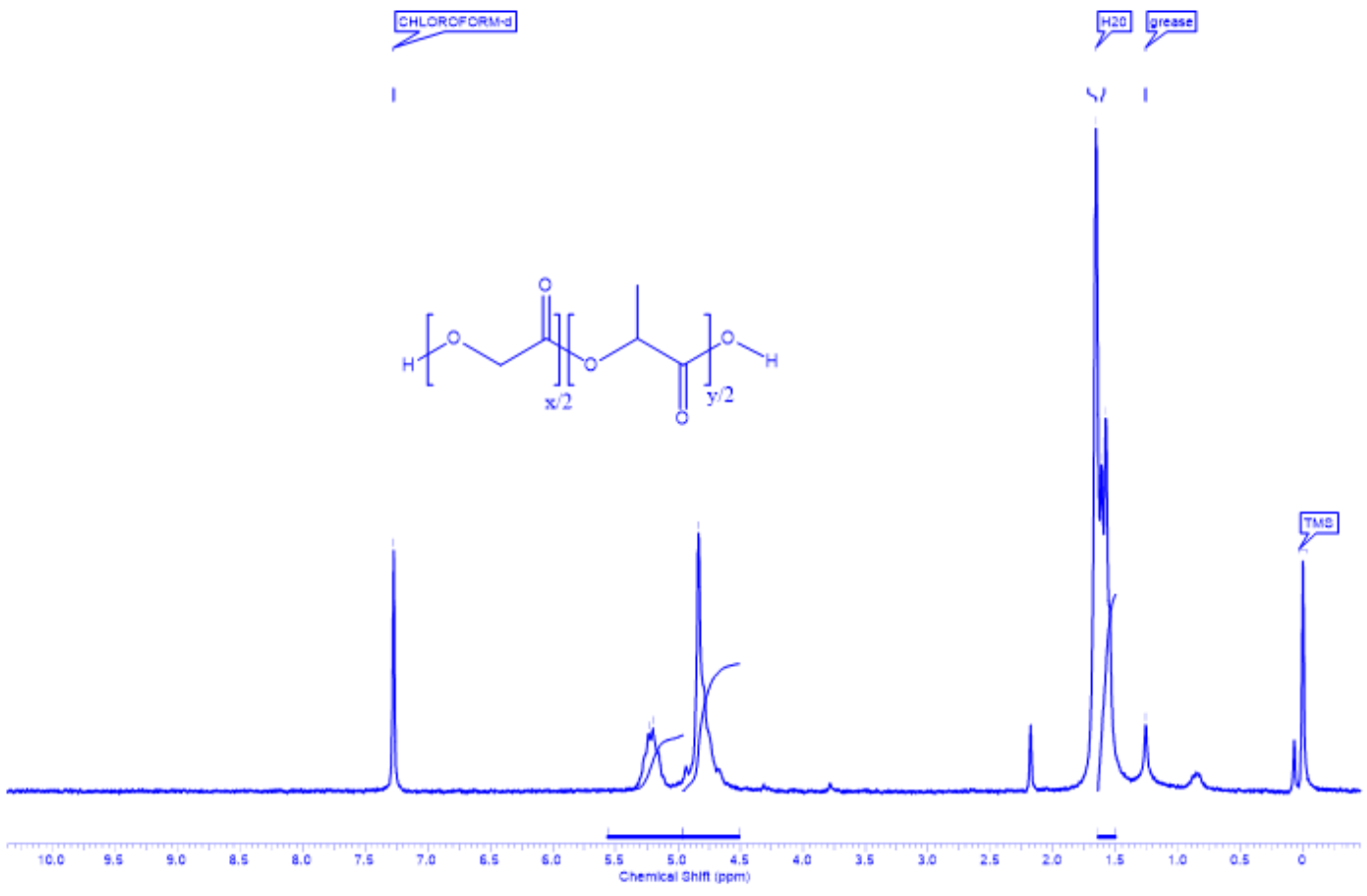

Figure 1

1H NMR of PLGA

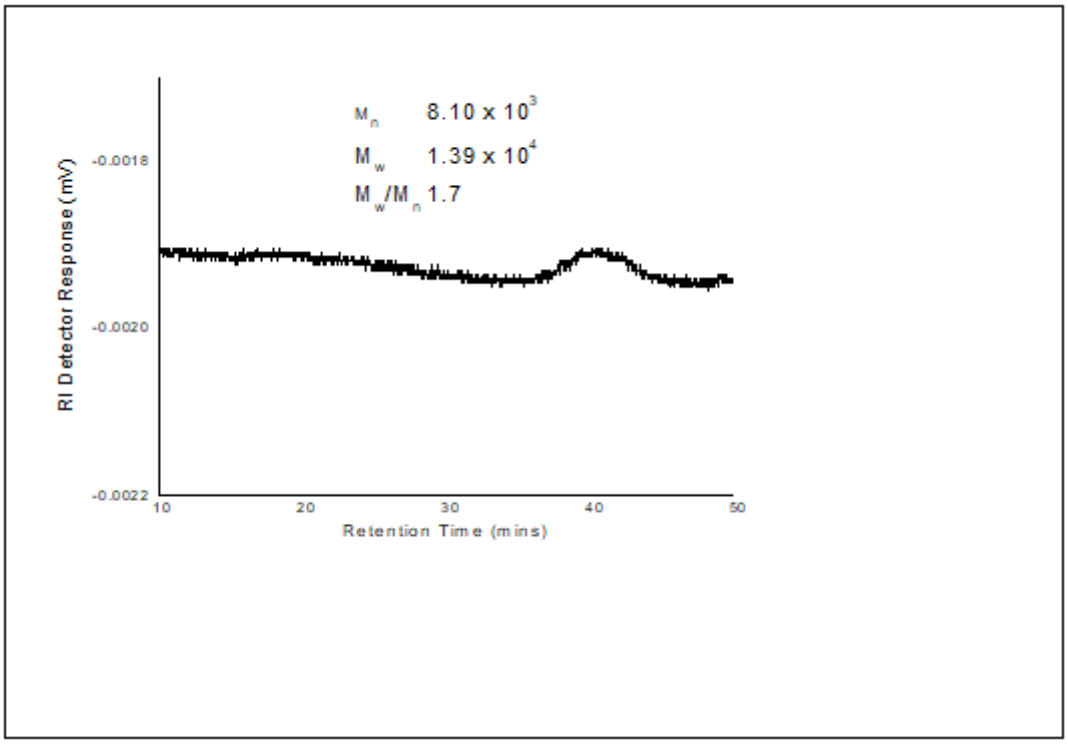

Figure 2

Size Exclusion Chromatography of PLGA

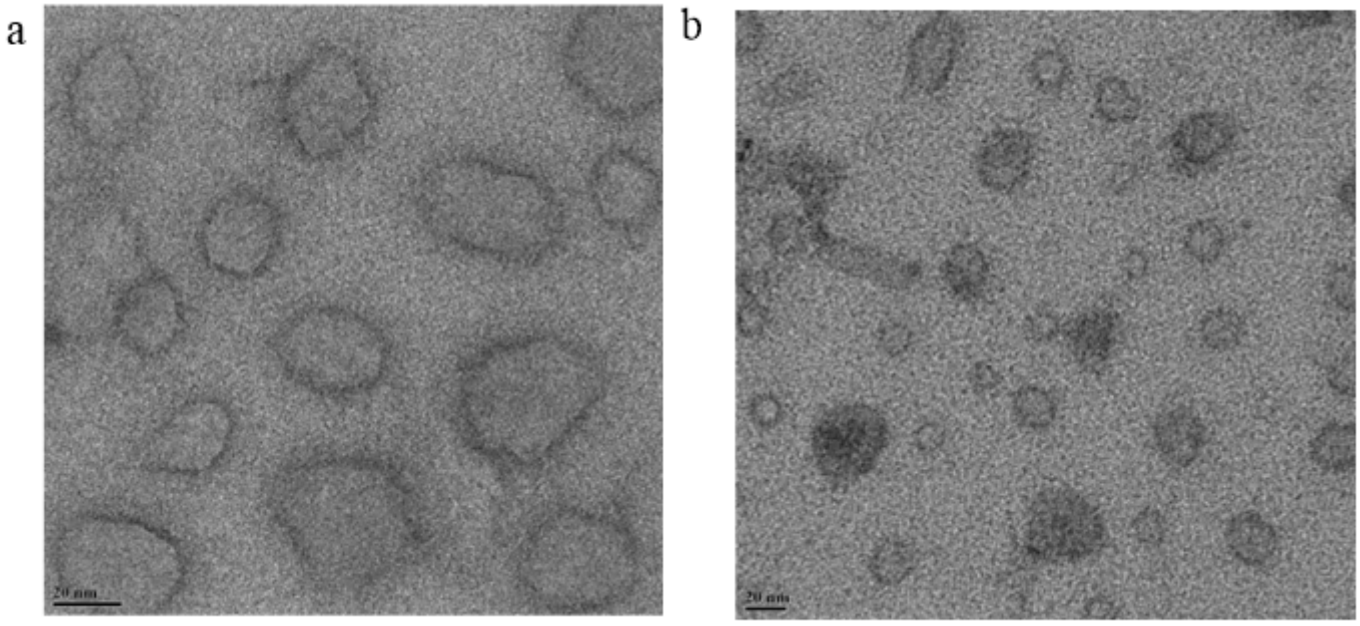

Figure 3

TEM analyses (a),P-DSPE-Ir and (b) P-DSPE- PEG-Ir (scale bar for both images 20 nm)

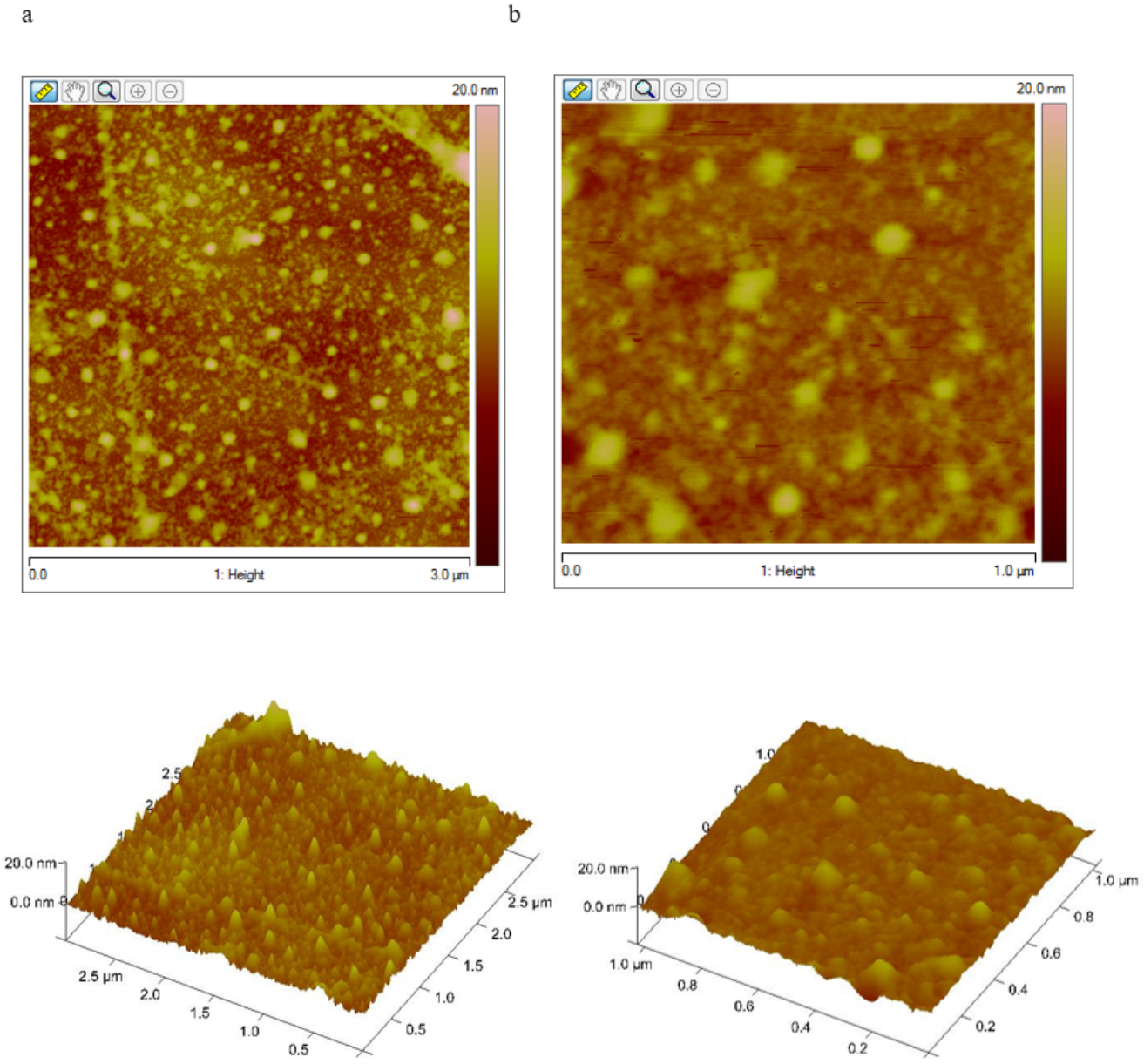

Figure 4

AFM analyses (a)P-DSPE-Ir (3 micron scale and 20 nm is the scale bar)and (b) P-DSPE- PEG-Ir (1 micron scale and 20 nm is the scale bar)

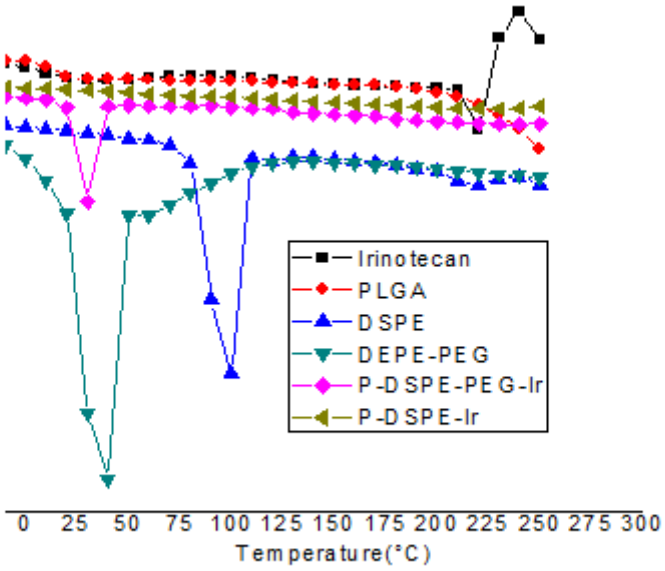

Figure 6

Differential scanning calorimetery analysis of LPs

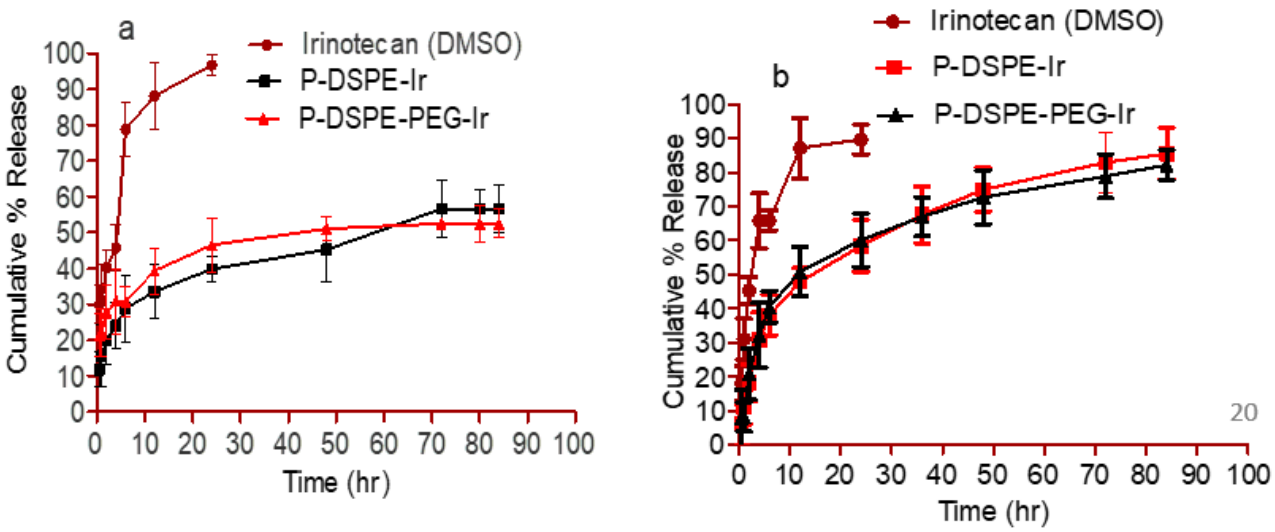

Figure 7

LPs were dialyzed against 1% (w/v) Tween® 80 in phosphate buffered saline (a)PBS, pH 7.4 , and (b) 50% fetal calf serum

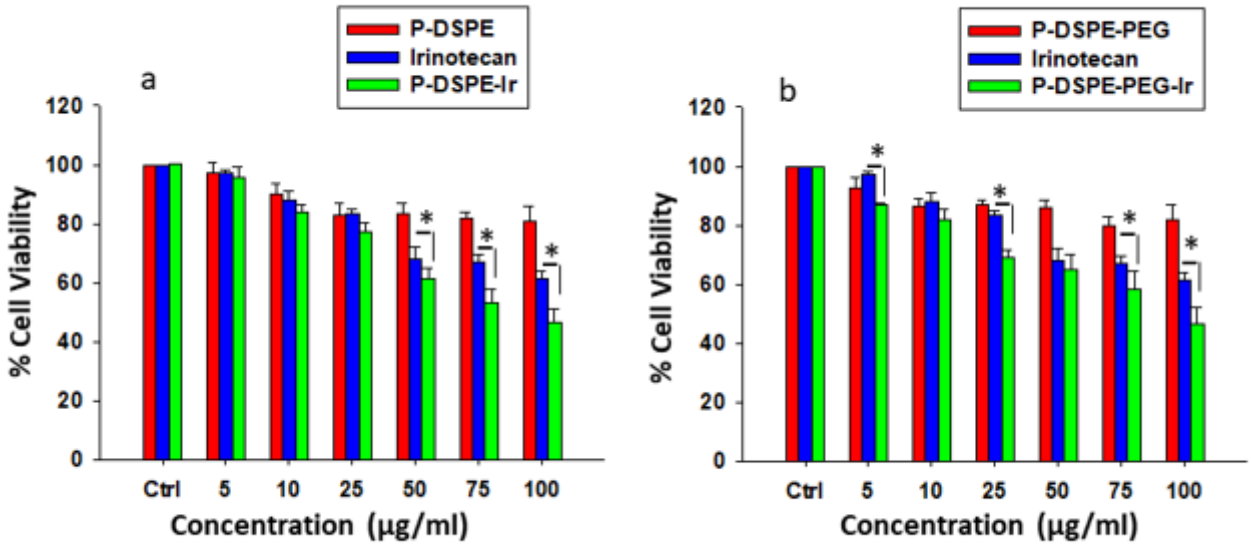

Figure 8

Cell viability of CT-26 cells in the presence of Ir nanoformulation (a)P-DSPE-Ir (b)P-DSPE-PEG-Ir, Cell viability was expressed as a percentage of control untreated cells (n = 5, * indicates P value ≤0.05)

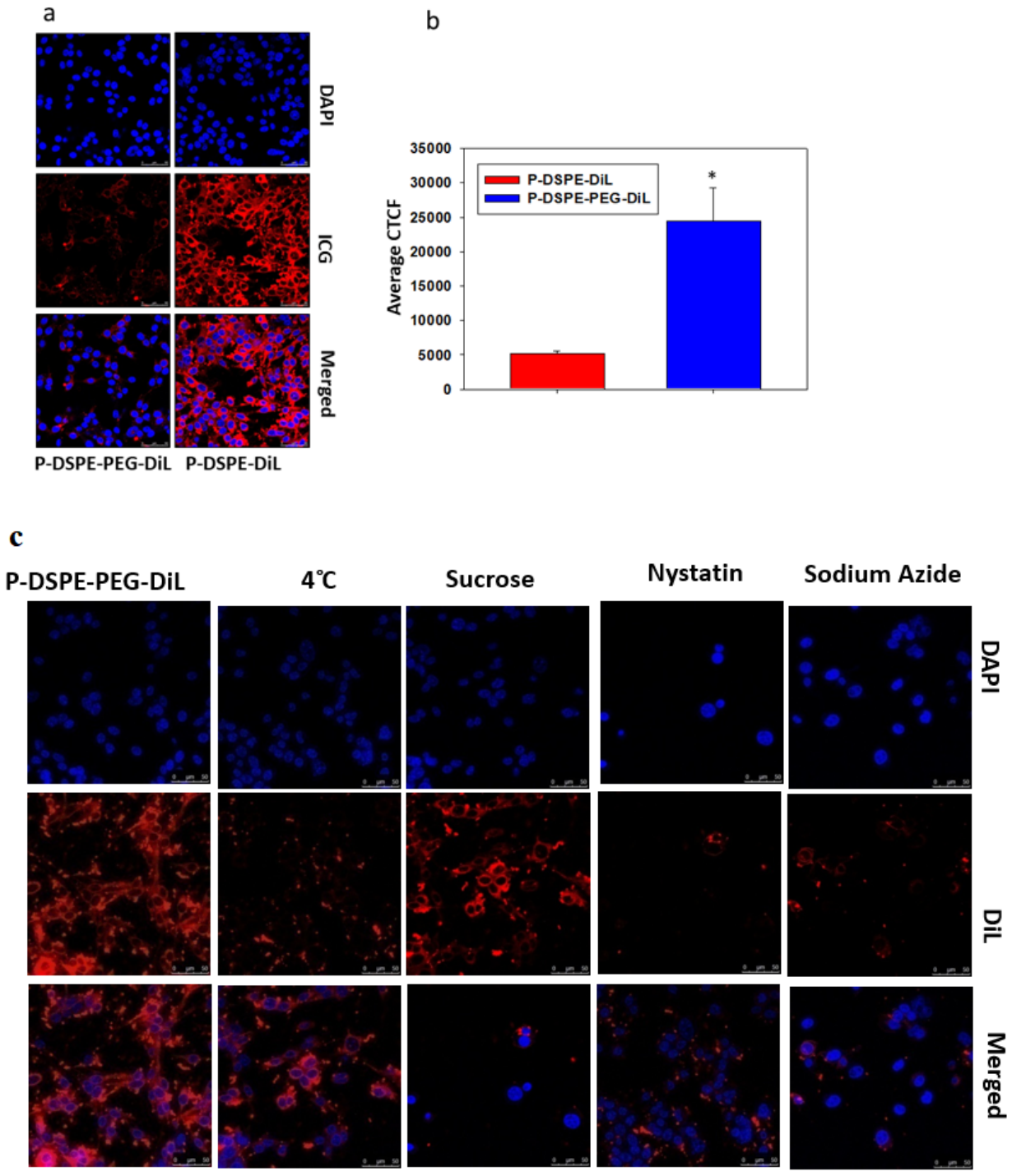

Figure 9

Cellular uptakes of LPs (a)confocal laser scanning microscopy (CLSM) Qualitative and (b) Quantitative uptake of LPs (c)Cellular uptake pathway analysis

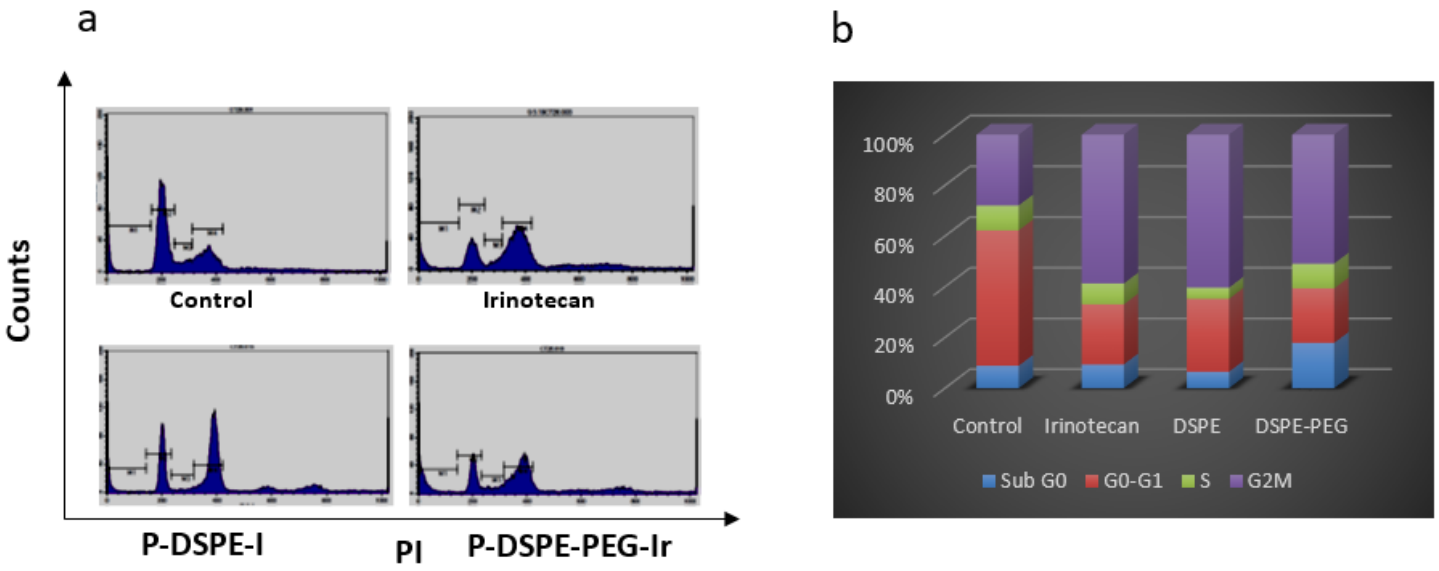

Figure 10

Cell cycle analyses (a) Qualitative histogram of cell cycle analysis and (b) Quantification of cell in each phase of cancer cell

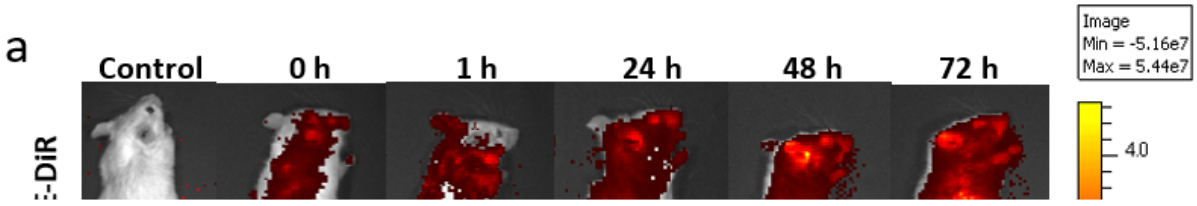

Figure 11

In vivo and Ex Vivo Biodistribution Studies (a) Whole body in vivo image obtained at 0,1,4,24,48 and 72 hr (b) Ex vivo image of excised organ at 72 h (c) Ex vivo quantification of fluorescence.

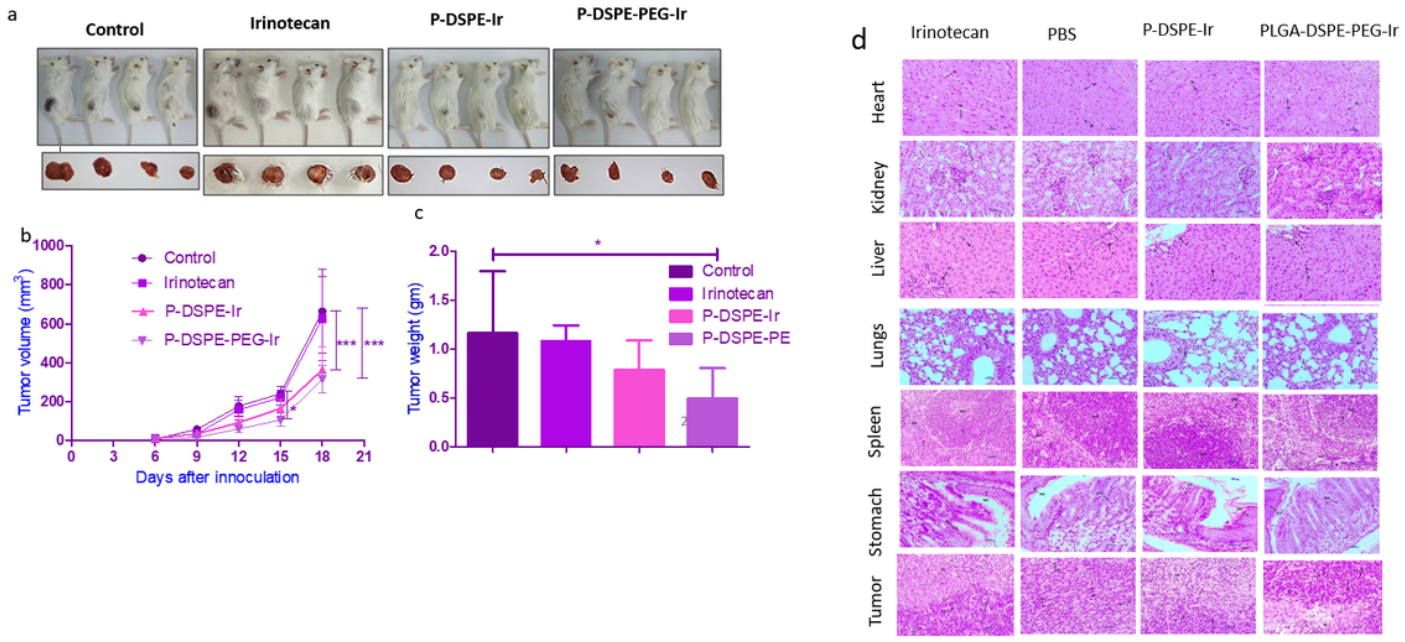

Figure 12

In vivo tumor site retention study representative images for an animal used in study (a) Images of mice with tumor for different treatment group (scale bar 20 um), (b) average tumor volume (c), average tumor weight and (d)Histopathology after tumor therapy (statistical analysis indicates * P value ≤0.05, ** P value ≤0.01, *** P value ≤0.001)

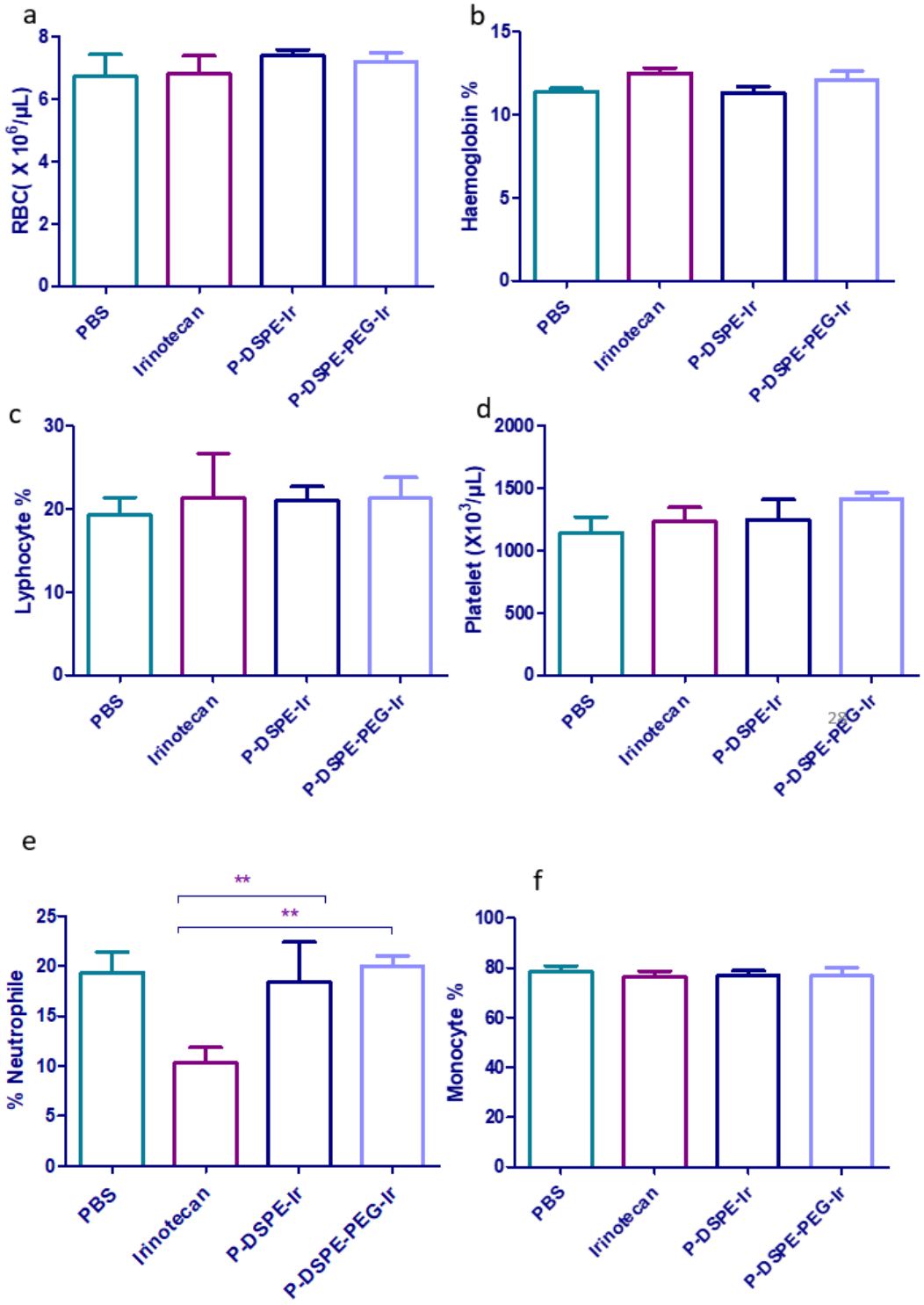

Figure 13

Haematological parameter for In vivo toxicity study (a-f, statistical analysis indicates * P value ≤0.05, ** P value ≤0.01, *** P value ≤0.001)

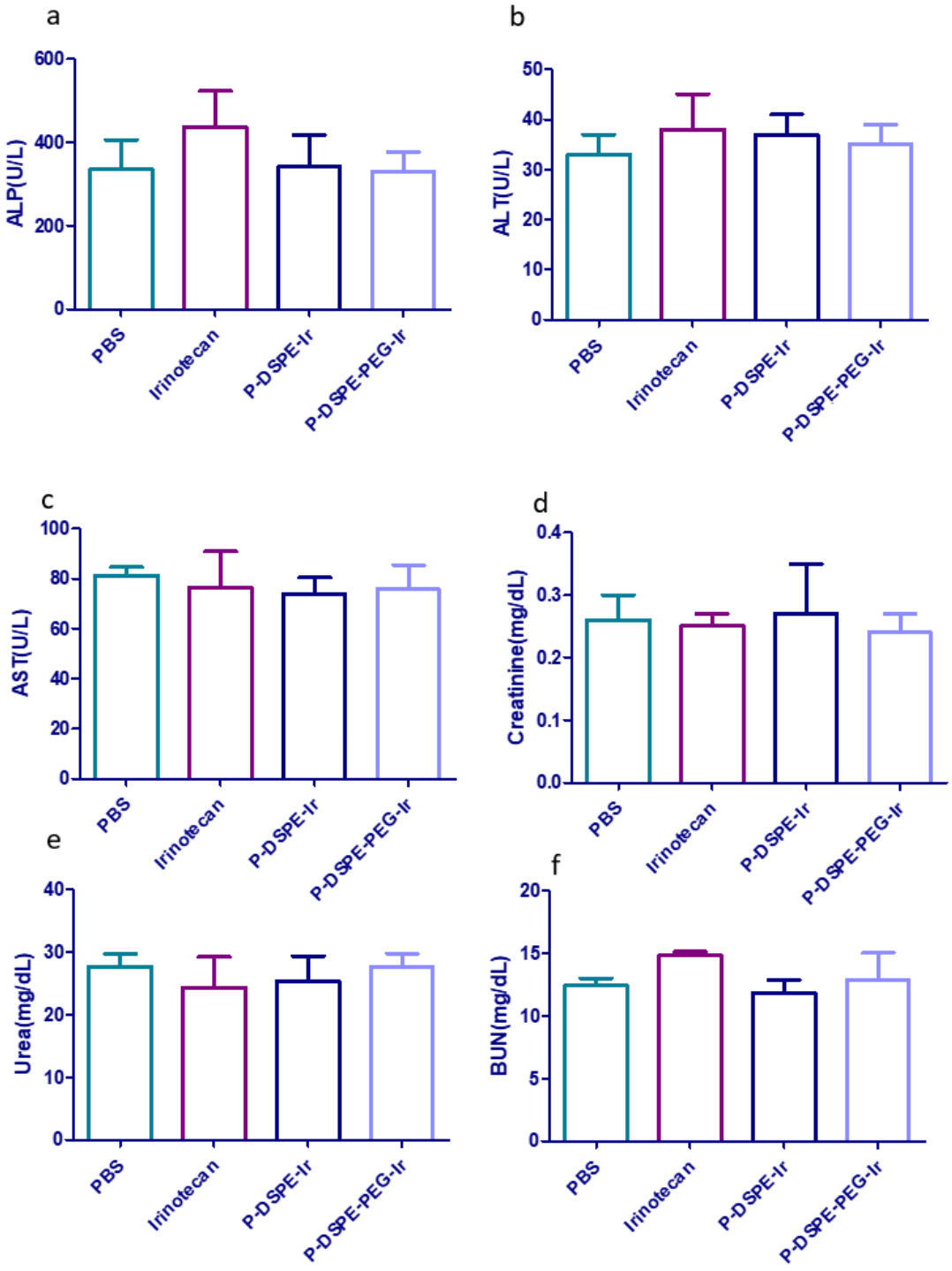

Figure 14

Biomarker analysis for In vivo toxicity study (a-f)

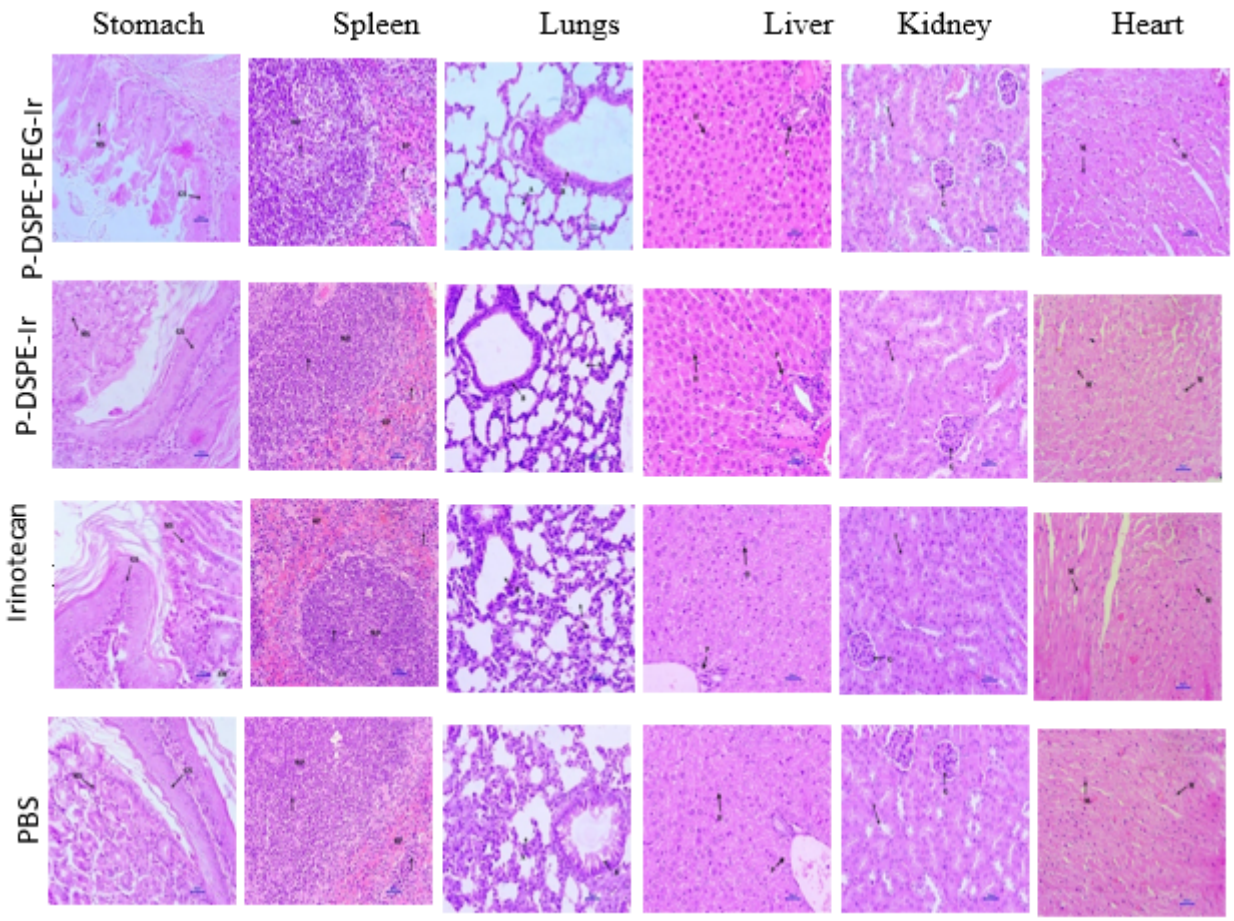

Figure 15

Histopathological analysis for In-vivo toxicity study for PBS, Ir, and P-DSPE-Ir and P-DSPE-PEG-Ir (scale bar 20 um)

Supplementary Files

This is a list of supplementary files associated with this preprint. Click to download.

- GraphicalAbstract.png
- SupportingInformation.docx
- Scheme1.png
- Scheme2.png